

# A stochastic approach to the quantum noise of a single-emitter nanolaser

Matias Bundgaard-Nielsen,<sup>1,2</sup> Emil Vosmar Denning,<sup>1,2,3</sup> Marco Saldutti,<sup>1,2</sup> and Jesper Mørk<sup>1,2</sup>

<sup>1</sup>*Department of Electrical and Photonics Engineering,*

*Technical University of Denmark, Building 343, 2800 Kongens Lyngby, Denmark*

<sup>2</sup>*NanoPhoton-Center for Nanophotonics, Technical University of Denmark, Building 343, 2800 Kongens Lyngby, Denmark*

<sup>3</sup>*Nichtlineare Optik und Quantenelektronik, Institut für Theoretische Physik, Technische Universität Berlin, Berlin, Germany*

(Dated: January 30, 2023)

It is shown that the intensity quantum noise of a single-emitter nanolaser can be accurately computed by adopting a stochastic interpretation of the standard rate equation model under the only assumption that the emitter excitation and photon number are stochastic variables with integer values. This extends the validity of rate equations beyond the mean-field limit and avoids using the standard Langevin approach, which is shown to fail for few emitters. The model is validated by comparison to full quantum simulations of the relative intensity noise and second-order intensity correlation function,  $g^{(2)}(\tau)$ . Surprisingly, even when the full quantum model displays vacuum Rabi oscillations, which are not accounted for by rate equations, the intensity quantum noise is correctly predicted by the stochastic approach. Adopting a simple discretization of the emitter and photon populations, thus, goes a long way in describing quantum noise in lasers. Besides providing a versatile and easy-to-use tool for modeling a new generation of nanolasers with many possible applications, these results provide insight into the fundamental nature of quantum noise in lasers.

The ability of a laser to generate a coherent optical signal with ultra-low noise is key to a wide range of applications, including the internet [1], sensors [2], as well as fundamental tests of physics, including the detection of gravitational waves [3]. Recent advancements in nanotechnology have enabled the realization of a new generation of microscopic lasers, for instance, based on semiconductor quantum dots in photonic crystals [4–6], opening new possibilities in, e.g., on-chip communications [7–10] and quantum technology [11]. However, as the laser shrinks into the microscopic regime, the power diminishes, and the intrinsic quantum noise of the laser may well be the limiting factor. The noise of lasers is a rich and complex field which is still developing [12–22]. For few emitters, it is, in principle, possible to perform full-scale quantum simulations of the noise properties [23–27]. However, such simulations are numerically demanding, add little insight into the physics, and it is difficult to design laser structures with optimal properties directly based on this approach. Rather, the use of rate equations has proven extremely successful in realizing the advanced modern semiconductor laser of today [28]. However, rate equations are derived in the mean-field limit, which we show is not valid for few emitters, even if stochastic Langevin noise terms are included [29].

In this paper, we consider the ultimate limit of a nanolaser, where the gain medium is a single-emitter, e.g., a quantum dot in a photonic crystal cavity as studied in [30, 31], and shown in Fig. 1. We show that the quantum noise of such nanolasers can be quantitatively described by classical rate equations by adopting a simple stochastic interpretation with discrete population changes [14, 15, 32, 33]. This is surprising since rate equations are derived in a mean-field limit and neglect coherent emitter-photon interactions. We find excellent

agreement with full quantum mechanical master eqs. regarding the intensity noise, even in the regime where vacuum Rabi oscillations manifest. The appearance of sub-Poissonian statistics below threshold is also predicted by our approach, while standard Langevin approaches fail in this regime.

Our finding enables a new approach towards the quantum noise of nanolasers. Not only does it provide an intuitive and simple simulation tool, but it also offers new insights into the origin of quantum noise in lasers.

In second quantization, the single-emitter laser is described by a master equation of the form [23, 24]:

$$\frac{\partial \rho}{\partial t} = -\frac{i}{\hbar}[H, \rho] + \kappa \mathcal{D}_a[\rho] + \gamma_D \mathcal{D}_{\sigma^\dagger \sigma}[\rho] + \gamma_A \mathcal{D}_\sigma[\rho] + P \mathcal{D}_{\sigma^\dagger}[\rho] \quad (1)$$

where  $H = -\hbar \Delta a^\dagger a + \hbar g(\sigma^\dagger a + a^\dagger \sigma)$  is the Jaynes-Cummings Hamiltonian with  $g = \sqrt{d^2 \omega_{eg} / (2\hbar \epsilon_0 \epsilon V)}$  being the light-matter coupling [34]. Here  $d$  is the emitter dipole moment,  $\epsilon$  is the dielectric constant of the background material,  $V$  is the cavity mode volume,  $\sigma = |g\rangle \langle e|$  is the atomic transition operator,  $a$  is the cavity mode annihilation operator,  $\Delta = \omega_{eg} - \omega_c$  is the detuning between the electronic transition  $\omega_{eg}$  and the cavity frequency  $\omega_c$ , and  $\mathcal{D}_A[\cdot] = \frac{1}{2}(2A(\cdot)A^\dagger - (\cdot)A^\dagger A - A^\dagger A(\cdot))$  is the Lindblad operator. The various Lindblad terms describe dissipative processes relevant to single-emitter lasers;  $\kappa$  is the cavity decay rate,  $\gamma_D$  is the pure dephasing rate, arising from, e.g., phonons in quantum dot emitters [31],  $\gamma_A$  is the non-radiative decay and/or decay into non-lasing modes, and  $P$  is the pump rate of the emitter, modeled as incoherent pumping [23, 35]. The master equation is numerically implemented by using QuTIP [36, 37].

Under the assumption of a large dephasing rate, such that the polarization can be eliminated [31, 35, 38], a rate

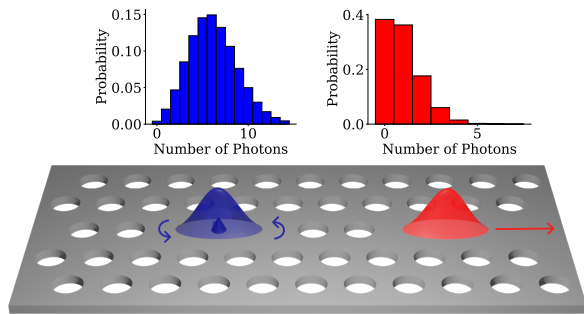


FIG. 1. Schematic of a photonic crystal cavity laser with a single quantum dot. Examples of photon distributions inside and outside the cavity, calculated with the stochastic approach, are shown above threshold for the same parameters as in Fig. 3 and 4.

equation can be derived from the master equation in eq. (1). With  $n_a = \langle a^\dagger a \rangle$  and  $n_e = \langle \sigma^\dagger \sigma \rangle$  and making a mean-field approximation we get:

$$\frac{dn_a}{dt} = \gamma_r(2n_e - 1)n_a + \gamma_r n_e - \kappa n_a \quad (2)$$

$$\frac{dn_e}{dt} = P n_g - \gamma_r(2n_e - 1)n_a - \gamma_r n_e - \gamma_A n_e \quad (3)$$

where an emitter-cavity coupling rate given by  $\gamma_r = 4g^2/(P + \kappa + \gamma_D + \gamma_A)$ . Since the polarization was adiabatically eliminated, this model does not display Rabi oscillations. Furthermore, the equations only govern the average emitter excitation and number of cavity photons and do not include quantum noise. Conventionally, quantum noise is accounted for by adding random Langevin forces to the RHS. of eqs. (2) and (3) [28]. As we shall see, however, this leads to incorrect results for the intensity correlation,  $g^{(2)}(0)$ , which has been recognized as essential in identifying the regime of lasing [12, 16].

Another approach to include noise in the rate equations is to interpret Eqs. (2) and (3) as a stochastic process for integer-valued variables,  $n_e$  and  $n_a$  [14, 33]. The stochastic approach was introduced for many emitters but is here applied to the case of a single-emitter. In essence, it replaces the rates in eqs. (2)-(3) by Poisson processes, thus attributing all the quantum noise of the laser to the discrete nature of photons and emitter excitation. Notably, this approach does not require the calculation of diffusion coefficients for Langevin forces, nor does it assume small perturbations around a steady state.

Here, to numerically solve the stochastic equation, we use Gillespies first-reaction method, which is numerically exact [15]. We choose parameters compatible with a single quantum dot in a photonic crystal cavity with a light-matter coupling of  $g = 0.1 \text{ ps}^{-1}$  [30] and a cavity decay rate  $\kappa = 0.02 \text{ ps}^{-1}$  [19]. Furthermore, we use

$\gamma_A = 0.012 \text{ ps}^{-1}$  and study three different pure dephasing rates  $\gamma_D = 0, 1, 10 \text{ ps}^{-1}$ . Ignoring pump broadening, this gives  $\beta$ -factors of  $\beta = \gamma_r/(\gamma_r + \gamma_A) = 0.999, 0.764, 0.249$ , thus placing the laser in the high- $\beta$  or "thresholdless" regime. It is worth noting that recent advances in dielectric nanocavities with deep subwavelength confinement [39–42] enable even larger values of  $g$ . Fig. 2 shows the results obtained from the master equation and the stochastic approach. The mean photon number  $n_a$ , the intensity correlation function  $g^{(2)}(0)$ , RIN, emission spectrum, and linewidth are depicted. See supplementary for details on calculations.

Fig. 2 (a,b,c) demonstrate excellent agreement between the stochastic approach and the master equation for the mean photon number, intensity correlation, and RIN. This is the case for all dephasing values and pump rates. The results of adding Langevin noise terms to eqs. (2) and (3) is also shown and we refer to [14] for details. It is clear that the Langevin approach captures the mean photon number and RIN relatively well, while there is a large deviation in the intensity correlation. This shows a fundamental problem of the Langevin approach for few emitters, since  $g^{(2)}(0)$  is a key measure of the statistics of the light [12, 13, 35]. Below threshold, the light is antibunched in the single-emitter case, which is correctly identified by  $g^{(2)}(0) < 1$  for the master equation and stochastic approach, while the Langevin approach predicts super-Poissonian statistics,  $g^{(2)}(0) > 1$ . Furthermore, surprisingly, the results produced by the stochastic approach are also correct in the "bad cavity limit" where  $\kappa > \gamma_D, \gamma_A$  (red curves) and the adiabatic approximation, which is at the heart of the rate equation approximation, breaks down.

Fig. 2(d) shows the emission spectrum for the case of  $\gamma_D = 0$ . Note that the stochastic approach, which in its present form does not contain information about the phase, cannot calculate the emission spectrum. In the emission spectrum, we observe two peaks for low pump values that reflect Rabi oscillations and correspondingly have a splitting of  $2g = 0.2 \text{ ps}^{-1}$ . As the pump rate is increased, we see the transition to lasing as the Rabi peaks coalesce into a single peak at the cavity frequency, whose linewidth narrows significantly. This is seen from Fig. 2(e) which shows the corresponding linewidth  $\Delta\nu$  (FWHM) calculated from the Liouville gap (the smallest real eigenvalue in the system) [16].

In contrast to macroscopic lasers, characterized by  $\beta \ll 1$ , the transition to lasing in nanolasers with  $\beta$  of order unity, does not show a clear phase transition [43], giving rise to vivid discussion of the proper definition of threshold [18, 44–46]. This highlights the ambiguity in defining the threshold for nanolasers, in contrast to the case of macroscopic lasers. In Fig. 2(d,e) vertical lines show the prediction of two threshold definitions,  $P_{pr}$  and  $P_{cl}$ , to be further discussed below. In both expressions, the number of carriers at lasing threshold,  $n_{e,th}$ ,

is defined by the balance between gain and cavity loss  $\gamma_r(2n_{e,th} - 1) = \gamma_c$ . From here, the classical approach [28] is to compute the corresponding pump rate by assuming that the photon population below threshold is zero. This procedure leads to the following expression, where we have ignored pump broadening [47]

$$P_{cl} = \left( \frac{2}{1 - 1/(2\xi)} \right) \frac{1}{2} \frac{\gamma_c}{\beta} (1 + 2\xi) \quad (4)$$

with  $\xi = \gamma_r/(2\gamma_c)$ . However, in the presence of a near-unity  $\beta$ -factor, the number of photons below transparency may be non-negligible [48]. At the same time, if  $\gamma_r$  is sufficiently larger than  $\kappa$ , a generated photon has a significant chance of being re-absorbed rather than escaping the cavity. This cycle of spontaneous emission into the lasing mode and stimulated re-absorption, i.e. photon recycling [47, 48], may effectively increase the carrier lifetime and lower the pump rate required to reach the lasing threshold. By including the effect of photon recycling, one arrives at the following expression [47]:

$$P_{pr} = \left( \frac{2}{1 - 1/(2\xi)} \right) \frac{1}{2} \frac{\gamma_c}{\beta_{eff}}, \quad \beta_{eff} = \frac{\beta}{1 + 2\xi(1 - \beta)} \quad (5)$$

It is seen that  $P_{pr}$  marks the pump value at which the Rabi peaks coalesce,  $g^{(2)}(0)$  approaches 1 from below, and also the linewidth starts narrowing. At the pump value of  $P_{cl}$ , the linewidth has reduced significantly and one enters a regime with  $g^{(2)}(0) \approx 1$ , independently of the pump value. At a critical pump value, denoted as the quenching threshold and indicated by  $P_{qn}$ , the linewidth starts to rebroaden, and  $g^{(2)}(0)$  quickly approaches the thermal value of 2. This quenching behavior at high pump values is in agreement with previous work [23, 24, 35] and occurs because pump-induced dephasing dominates the emitter broadening. See supplementary for details on  $P_{qn}$  and also analytical expressions for the linewidth, which are compared to the simulations of the master equation in Fig. 2(e).

Reaching the classical threshold requires a larger pump rate compared to the photon recycling threshold. Therefore, the photon number is larger, and the linewidth has narrowed significantly. The photon recycling threshold, however, reliably marks the pump rate at which the linewidth starts to narrow, and the photon statistics change from anti-bunched to the thermal regime with super-Poissonian statistics preceding lasing. This feature becomes particularly clear when various light-matter coupling rates (not shown here) are considered. Conversely, the classical threshold would not mark a consistent stage in the evolution toward coherent laser light.

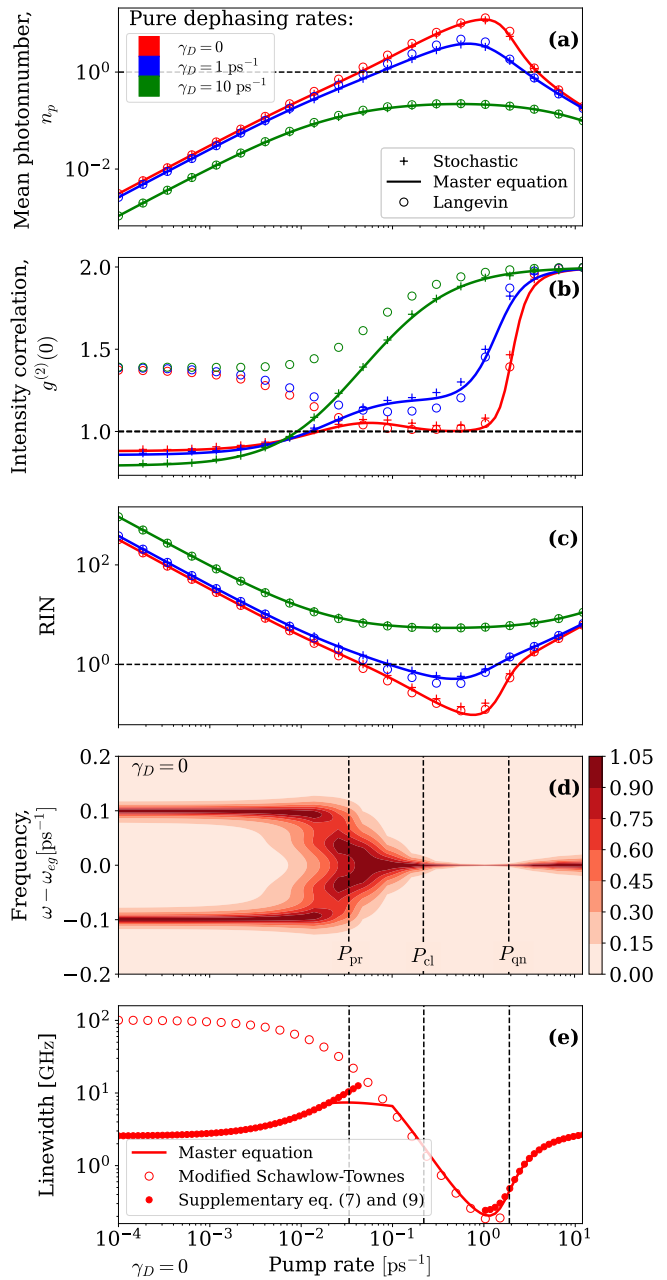


FIG. 2. (a) Cavity population, (b) second-order correlation function  $g^{(2)}(0)$ , (c) RIN, (d) emission spectrum, and (e) linewidth vs. pump-rate, for three different pure dephasing rates:  $\gamma_D = 0$  (red),  $\gamma_D = 1 \text{ ps}^{-1}$  (blue), and  $\gamma_D = 10 \text{ ps}^{-1}$  (green). The spectrum is only shown for  $\gamma_D = 0$ , normalized to 1 for each pump rate, and is calculated using the master equation. The characteristic pump rates,  $P_{re}$ ,  $P_{cl}$ , and  $P_{qn}$  separate the laser into four qualitatively different regimes I-IV.

To further characterize the quantum noise, we consider the frequency dependence of the RIN spectrum. The spectrum of the outcoupled signal is the experimentally relevant observable and differs qualitatively from the intra-cavity spectrum due to the non-trivial action of

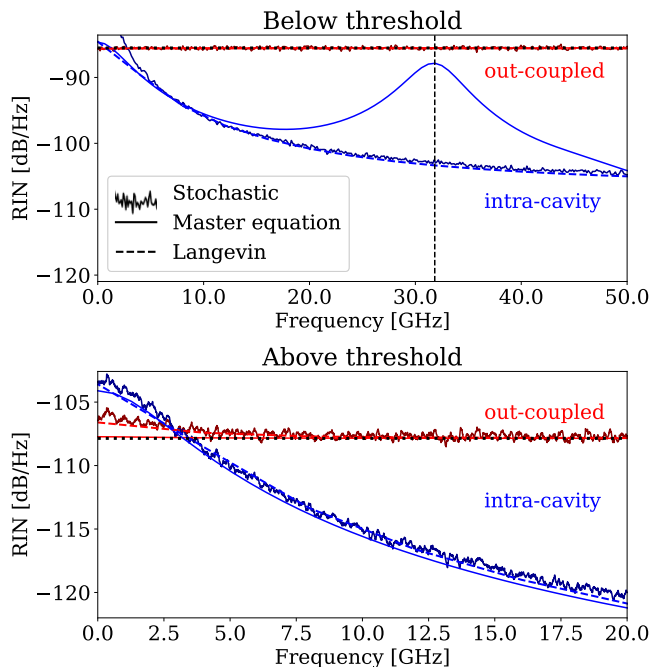


FIG. 3. RIN spectra for intra-cavity and outcoupled photons, below and above threshold. The RIN is calculated by the master equation, stochastic approach, and the analytic Langevin approach. The parameters are the same as in Fig. 2 with  $P = 0.0012 \text{ ps}^{-1}$  and  $P = 0.3023 \text{ ps}^{-1}$  in respectively below and above threshold. The detector integration times are  $T = \gamma_r^{-1} = 0.83 \text{ ps}^{-1}$  and  $8.36 \text{ ps}^{-1}$  respectively, the vertical dashed line shows the Rabi frequency at  $f = 2g/2\pi = 31.8 \text{ GHz}$ , and the horizontal dots mark the standard quantum limit.

the outcoupling mirror [49]. This is illustrated in Fig. 1, where the photon distribution changes drastically outside the cavity. We calculate the outcoupled noise spectrum by simulating the detection of photons outside the cavity with an integration time  $T$ . In the master equation, this is done using normally ordered photodetection theory [23, 50–52], and for the stochastic approach, we track all outcoupling events [32]; see supplementary material for details. In the calculations, we choose a detector integration time small enough to capture all features in the outcoupled spectrum. Empirically, the inverse emission rate  $\gamma_r^{-1}$  is a good choice.

Fig. 3 shows RIN spectra for the intra-cavity and outcoupled photons for two pump values: one below threshold and one above. We also show results based on the analytic Langevin approach introduced in ref. [28] and adopted to the nanolaser rate eqs. in ref. [32]. Below threshold, Rabi oscillations manifest themselves in the intra-cavity RIN spectrum calculated by the master equation as a peak around  $2\pi f = 2g$ . These oscillations arise due to the dynamics of the atomic po-

larization, which neither the Langevin approach nor the stochastic rate equation approach can capture, due to the adiabatic elimination carried out in the rate equations [15, 32]. Considering the outcoupled RIN instead, we see that the noise is dominated heavily by the partition noise at the cavity mirrors [28] and it is accurately given by the standard quantum limit:  $\text{SN} = 2/(n_a\kappa)$ , without any features of Rabi oscillations.

Above threshold, Rabi oscillations do not manifest themselves in the RIN spectrum, and all three approaches agree. We again see that the shot noise stemming from the cavity mirrors dominates the outcoupled RIN spectrum. Note, however, that the outcoupled RIN spectrum is not simply given by the intra-cavity RIN spectrum with the added shot noise. Below 5 GHz, the outcoupled RIN is thus smaller than the intra-cavity RIN [28, 32]. While outcoupling at the laser mirror introduces quantization (shot) noise of the outcoupled photons, the noise is reduced at low frequencies due to anti-correlation effects [28, 32]. The partition noise at the cavity mirrors can thus lower the noise for low frequencies.

We now consider the time-dependency of the intra-cavity intensity correlation function,  $g^2(\tau)$  (see supplementary). The results can be seen in Fig. 4, where we see deviations between the stochastic approach and the master equation below and above threshold. The deviation below threshold clearly arises from Rabi oscillations, which, as mentioned, cannot be captured by the stochastic approach. Above threshold, the absolute deviation is quite small (within 1-2%), but the qualitative behavior is significantly different. Although not visible in the spectrum, transitions in the Jaynes-Cummings Ladder still affect the two-time correlation function. We thus find that the master eq. results can be well fitted by the following expression derived in [26]:

$$g^{(2)}(\tau) = 1 + d_1 \exp(-\tau/\tau_c) + \sum_{m=1}^{m=3} c_m \cos(\omega_m \tau) e^{-\tau/\tau_m} \quad (6)$$

Here,  $\tau_c^{-1} = \kappa - P/4g^2$  is the coherence time for the non-oscillating term, and  $d_1$ ,  $c_m$ ,  $\omega_m$ , and  $\tau_m$  are fitted.  $\omega_m$  is fitted to values of  $\omega_1 \approx g$ ,  $\omega_2 \approx 2g\sqrt{2}$ , and  $\omega_3 \approx 2g\sqrt{4}$  which corresponds to the following transitions in the Jaynes-Cummings ladder:  $|1, +\rangle \rightarrow |g, 0\rangle$ ,  $|1, +\rangle \rightarrow |1, -\rangle$ , and  $|3, +\rangle \rightarrow |3, -\rangle$  respectively, where we here defined  $|n, \pm\rangle = (|g\rangle |n+1\rangle \pm |e\rangle |n\rangle)/\sqrt{2}$  [53]. The oscillating terms, thus, stem from Rabi oscillations and play the same role as the correction  $\delta g^{(2)}(\tau)$  to the Siegert relation found in ref. [54], where they write:  $g^{(2)}(\tau) = 1 + |g^{(1)}(\tau)|^2 + \delta g^{(2)}(\tau)$ . They show that the correction  $\delta g^{(2)}(\tau)$  is necessary when either strong emitter-emitter or emitter-photon correlations are present. We find a similar result. Only including the non-oscillating term with coherence time  $\tau_c$ , i.e.  $g^{(2)}(\tau) = 1 + (g^{(2)}(0) - 1)e^{-\tau/\tau_c}$ , is sufficient to describe  $g^{(2)}(\tau)$  as obtained from the stochastic approach. The stochastic approach, how-

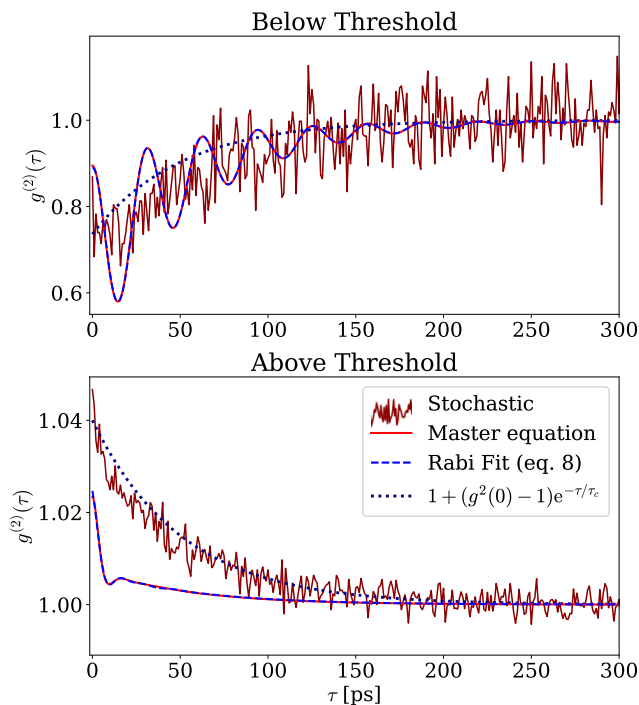


FIG. 4. Computed correlation function  $g^{(2)}(\tau)$  below and above the laser threshold for the same parameters as in Fig. 2 and 3. A fit to the master equation with the expression (6) is also shown, as well as a monotonically decaying exponential with coherence lifetime  $\tau_c^{-1} = \kappa - P/4g^2$ .

ever, cannot capture the shorter-lived Rabi oscillations with  $\tau_m \approx 1/(5\kappa)$ , leading to the master equation initially decaying much faster and thus explaining the deviation.

In conclusion, we have shown that a simple stochastic interpretation [15] of standard rate equations accurately accounts for the intensity quantum noise of a single-emitter laser. In contrast, the conventional Langevin approach [28] breaks down, implying that the intensity quantum noise of a laser originates solely from the discrete nature of photon and emitter excitations. We also analyze the single-emitter lasing transition in detail and compare two definitions of the lasing threshold. The stochastic simulations can easily be extended to multiple emitters [14, 47], where quantum master equations become too numerically demanding. Our findings may, therefore, facilitate the analysis and design of a new generation of nanolasers while also allowing for a fundamental understanding of quantum noise.

#### ACKNOWLEDGEMENTS

This work was supported by the Danish National Research Foundation through NanoPhoton - Center for

Nanophotonics, Grant No. DNR147. EVD acknowledges support from Independent Research Fund Denmark through an International Postdoc fellowship, grant no. 0164-00014B.

- 
- [1] C. Z. Ning, *Advanced Photonics* **1**, 014002 (2019).
  - [2] R. M. Ma and R. F. Oulton, *Nature Nanotechnology* **14**, 12 (2019).
  - [3] B. P. Abbott and et. al., *Physical Review Letters* **116**, 061102 (2016).
  - [4] M. Notomi, *Reports on Progress in Physics* **73**, 096501 (2010).
  - [5] Y. Ota, M. Kakuda, K. Watanabe, S. Iwamoto, and Y. Arakawa, *Optics Express* **25**, 19981 (2017).
  - [6] M. Saldutti, M. Xiong, E. Dimopoulos, Y. Yu, M. Gioannini, and J. Mørk, *Nanomaterials* **11**, 3030 (2021).
  - [7] J. Shapiro, H. Yuen, and A. Mata, *IEEE Transactions on Information Theory* **25**, 179 (1979).
  - [8] B. E. Saleh and M. C. Teich, *Proceedings of the IEEE* **80**, 451 (1992).
  - [9] M. Notomi, K. Nozaki, A. Shinya, S. Matsuo, and E. Kuramochi, *Optics Communications* **314**, 3 (2014).
  - [10] D. A. Miller, *Journal of Lightwave Technology* **35**, 346 (2017).
  - [11] C. Weedbrook, S. Pirandola, R. García-Patrón, N. J. Cerf, T. C. Ralph, J. H. Shapiro, and S. Lloyd, *Reviews of Modern Physics* **84**, 621 (2012).
  - [12] S. Kreinberg, W. W. Chow, J. Wolters, C. Schneider, C. Gies, F. Jahnke, S. Höfling, M. Kamp, and S. Reitzenstein, *Light: Science and Applications* **6**, 1 (2017).
  - [13] C. Gies, F. Gericke, P. Gartner, S. Holzinger, C. Hopfmann, T. Heindel, J. Wolters, C. Schneider, M. Florian, F. Jahnke, S. Höfling, M. Kamp, and S. Reitzenstein, *Physical Review A* **96**, 023806 (2017).
  - [14] J. Mørk and G. L. Lippi, *Applied Physics Letters* **112**, 1 (2018).
  - [15] E. C. André, J. Mørk, and M. Wubs, *Optics Express* **28**, 32632 (2020).
  - [16] N. Takemura, M. Takiguchi, and M. Notomi, *Journal of the Optical Society of America B* **38**, 699 (2021).
  - [17] I. E. Protsenko, A. V. Uskov, E. C. André, J. Mørk, and M. Wubs, *New Journal of Physics* **23**, 063010 (2021).
  - [18] A. M. Yacomotti, Z. Denis, A. Biella, and C. Ciuti, *Laser & Photonics Reviews* **17**, 2200377 (2023).
  - [19] E. Dimopoulos, A. Sakanas, A. Marchevsky, M. Xiong, Y. Yu, E. Semenova, J. Mørk, and K. Yvind, *Laser and Photonics Reviews* **16**, 2200109 (2022).
  - [20] M. A. Carroll, G. D'Alessandro, G. L. Lippi, G. L. Oppo, and F. Papoff, *Physical Review Letters* **126**, 063902 (2021).
  - [21] A. A. Vyshnevyy and D. Y. Fedyanin, *Physical Review Letters* **128**, 029401 (2022).
  - [22] M. A. Carroll, G. D'Alessandro, G. L. Lippi, G.-L. Oppo, and F. Papoff, *Physical Review Letters* **128**, 029402 (2022).
  - [23] Y. Mu and C. M. Savage, *Physical Review A* **46**, 5944 (1992).
  - [24] M. Löffler, G. M. Meyer, and H. Walther, *Phys. Rev. A* **55**, 3923 (1997).
  - [25] E. del Valle and F. P. Laussy, *Physical Review A* **84**,

- 043816 (2011).
- [26] A. V. Poshakinskiy and A. N. Poddubny, *Journal of Experimental and Theoretical Physics* **118**, 205 (2014).
- [27] J. P. Clemens, P. R. Rice, and L. M. Pedrotti, *Journal of the Optical Society of America B* **21**, 2025 (2004).
- [28] L. A. Coldren, S. W. Corzine, and M. L. Mašanović, *Optical Engineering*, 2nd ed., 2 (John Wiley & Sons, Inc., Hoboken, NJ, USA, 2012).
- [29] K. Roy-Choudhury and A. F. J. Levi, *Physical Review A* **81**, 013827 (2010).
- [30] M. Nomura, N. Kumagai, S. Iwamoto, Y. Ota, and Y. Arakawa, *Nature Physics* **6**, 279 (2010).
- [31] S. Strauf and F. Jahnke, *Laser and Photonics Reviews* **5**, 607 (2011).
- [32] J. Mørk and K. Yvind, *Optica* **7**, 1641 (2020).
- [33] G. P. Puccioni and G. L. Lippi, *Optics Express* **23**, 2369 (2015).
- [34] E. V. Denning, M. Bundgaard-Nielsen, and J. Mørk, *Physical Review B* **102**, 235303 (2020).
- [35] A. Moelbjerg, P. Kaer, M. Lorke, B. Tromborg, and J. Mørk, *IEEE Journal of Quantum Electronics* **49**, 945 (2013).
- [36] J. R. Johansson, P. D. Nation, and F. Nori, *Computer Physics Communications* **183**, 1760 (2012).
- [37] J. R. Johansson, P. D. Nation, and F. Nori, *Computer Physics Communications* **184**, 1234 (2013).
- [38] M. Lorke, T. Suhr, N. Gregersen, and J. Mørk, *Physical Review B - Condensed Matter and Materials Physics* **87**, 205310 (2013).
- [39] S. Hu and S. M. Weiss, *ACS Photonics* **3**, 1647 (2016).
- [40] H. Choi, M. Heuck, and D. Englund, *Physical Review Letters* **118**, 223605 (2017).
- [41] F. Wang, R. E. Christiansen, Y. Yu, J. Mørk, and O. Sigmund, *Applied Physics Letters* **113**, 241101 (2018).
- [42] M. Albrechtsen, B. Vosoughi Lahijani, R. E. Christiansen, V. T. H. Nguyen, L. N. Casses, S. E. Hansen, N. Stenger, O. Sigmund, H. Jansen, J. Mørk, and S. Stobbe, *Nature Communications* **13**, 6281 (2022).
- [43] P. R. Rice and H. J. Carmichael, *Physical Review A* **50**, 4318 (1994).
- [44] W. W. Chow, F. Jahnke, and C. Gies, *Light: Science & Applications* **3**, e201 (2014).
- [45] N. Takemura, M. Takiguchi, E. Kuramochi, A. Shinya, T. Sato, K. Takeda, S. Matsuo, and M. Notomi, *Physical Review A* **99**, 053820 (2019).
- [46] G. Lippi, T. Wang, and G. Puccioni, *Chaos, Solitons & Fractals* **157**, 111850 (2022).
- [47] M. Saldutti, Y. Yu, and J. Mørk, “Unpublished work,” (2023).
- [48] Y. Yamamoto and G. Björk, *Japanese Journal of Applied Physics* **30**, 2039 (1991).
- [49] Y. Yamamoto, S. Machida, and O. Nilsson, *Physical Review A* **34**, 4025 (1986).
- [50] H. J. Carmichael, *Journal of the Optical Society of America B* **4**, 1588 (1987).
- [51] M. A. M. Marte and P. Zoller, *Physical Review A* **40**, 5774 (1989).
- [52] H. Ritsch, *Quantum Optics: Journal of the European Optical Society Part B* **2**, 189 (1990).
- [53] C. Gerry and P. Knight, *Introductory Quantum Optics* (Cambridge University Press, 2004).
- [54] M. Drechsler, F. Lohof, and C. Gies, *Applied Physics Letters* **120**, 221104 (2022).